

Supporting Information

**Biomass to porous carbon in one step: Directly activated biomass
for high performance CO₂ storage**

Norah Balahmar, Abdul S. Al-Jumialy and Robert Mokaya*

University of Nottingham, University Park, Nottingham NG7 2RD, U. K.

E-mail: r.mokaya@nottingham.ac.uk (*R. Mokaya*)

Table S1. The ratio of peak intensity of the D-peak to G-peak (I_D/I_G) of directly activated or conventionally activated carbons derived from sawdust biomass.

Sample	I_D/I_G
SD2600D	0.78
SD2600	0.79
SD2700D	0.83
SD2700	0.81
SD2800D	0.84
SD2800	0.84
SD4800D	0.87
SD4800	0.86

Table S2. Textural properties and CO₂ uptake of directly activated or conventionally activated carbons derived from *Paeonia Lactiflora* biomass

Sample	Surface area ^a (m ² g ⁻¹)	Pore volume ^b (cm ³ g ⁻¹)	Pore size ^c (Å)	CO ₂ uptake ^d (mmol g ⁻¹)		
				0.15 bar	1 bar	20 bar
PLF2800D	2349 (1915)	1.48 (0.86)	8.5/11/20	0.9	3.9	17.5
PLF2800	1908 (1471)	1.20 (0.67)	8/11/20	0.6	2.8	16.0

The values in the parenthesis refer to: ^amicropore surface area and ^bmicropore volume. ^cPore size distribution maxima obtained from NLDFT analysis. ^dCO₂ uptake at 25 °C and various pressures (i.e., 0.15 bar, 1 bar and 20 bar).

Table S3. Textural properties and CO₂ uptake of directly activated or conventionally activated carbons derived from seaweed (*Sargassum fusiforme*).

Sample	Surface area ^a (m ² g ⁻¹)	Pore volume ^b (cm ³ g ⁻¹)	Pore size ^c (Å)	CO ₂ uptake ^d (mmol g ⁻¹)		
				0.15 bar	1 bar	20 bar
SW2600D	976 (692)	0.50 (0.27)	6/8/12	1.0	2.7	8.0
SW2600	1034 (923)	0.46 (0.37)	6/8/12	1.3	3.8	7.8
SW2700D	1986 (1350)	0.96 (0.53)	6/8/12/19	0.8	2.6	11.4
SW2700	1624 (1442)	0.73 (0.58)	6/8/9/12	1.2	4.2	12.4
SW2800D	3095 (1009)	1.68 (0.39)	6/8/12/24	0.5	2.2	13.5
SW2800	2085 (1667)	0.93 (0.66)	6/8/12/19	0.8	3.4	15.5

The values in the parenthesis refer to: ^amicropore surface area and ^bmicropore volume. ^cPore size distribution maxima obtained from NLDFT analysis. ^dCO₂ uptake at 25 °C and various pressures (i.e., 0.15 bar, 1 bar and 20 bar).

Table S4. CO₂ uptake of various porous carbons at 25 °C and 0.15 bar or 1 bar (Table adapted from ref. 41)

	CO ₂ uptake (mmol/g)		Reference
	1 bar	0.15 bar	
Sawdust-derived activated carbon	4.8	1.2	1
KOH-activated templated carbons	3.4	~1.0	2
Hierarchical porous carbon (HPC)	3.0	~0.9	3
Petroleum pitch-derived activated carbon	4.55	~1.0	4
Activated carbon spheres	4.55	~1.1	5
Phenolic resin activated carbon spheres	4.5	~1.2	6
Poly(benzoxazine-co-resol)-derived carbon	3.3	1.0	7
Fungi-derived activated carbon	3.5	~1.0	8
Chitosan-derived activated carbon	3.86	~1.1	9
Polypyrrole derived activated carbon	3.9	~1.0	10
Soya bean derived N-doped activated carbon	4.24	1.2	11
N-doped ZTCs	4.4	~1.0	12
Activated templated N-doped carbon	4.5	1.4	13
Polyaniline derived activated carbon	4.3	1.38	14
N-doped activated carbon monoliths	5.14	1.25	15
Activated N-doped carbon	3.2	1.5	16
Activated hierarchical N-doped carbon	4.8	1.4	17
Activated N-doped carbon from algae	4.5	~1.1	18

1. M. Sevilla and A. B. Fuertes, *Energy Environ. Sci.*, 2011, **4**, 1765.
2. M. Sevilla and A. B. Fuertes, *J. Colloid Interface Sci.*, 2012, **366**, 147.
3. G. Srinivas, V. Krungleviciute, Z. X. Guo and T. Yildirim, *Energy Environ. Sci.*, 2014, **7**, 335.
4. J. Silvestre-Albero, A. Wahby, A. Sepulveda-Escribano, M. Martinez-Escandell, K. Kaneko and F. Rodriguez-Reinoso, *Chem. Commun.*, 2011, **47**, 6840.
5. N. P. Wickramaratne and M. Jaroniec, *ACS Appl. Mater. Interfaces*, 2013, **5**, 1849.
6. N. P. Wickramaratne and M. Jaroniec, *J. Mater. Chem. A*, 2013, **1**, 112.
7. G. P. Hao, W. C. Li, D. Qian, G. H. Wang, W. P. Zhang, T. Zhang, A. Q. Wang, F. Schuth, H. J. Bongard and A. H. Lu, *J. Am. Chem. Soc.*, 2011, **133**, 11378.
8. J. Wang, A. Heerwig, M. R. Lohe, M. Oschatz, L. Borchardt and Stefan Kaskel, *J. Mater. Chem.*, 2012, **22**, 13911.
9. X. Fan, L. Zhang, G. Zhang, Z. Shu, J. Shi, *Carbon*, 2013, **61**, 423.
10. M. Sevilla, P. Valle-Vigon and A. B. Fuertes, *Adv. Funct. Mater.*, 2011, **21**, 2781.
11. W. Xing, C. Liu, Z. Y. Zhou, L. Zhang, J. Zhou, S. P. Zhuo, Z. F. Yan, H. Gao, G. Q. Wang and S. Z. Qiao, *Energy Environ. Sci.*, 2012, **5**, 7323.
12. Y. D. Xia, R. Mokaya, G. S. Walker and Y. Q. Zhu, *Adv. Energy Mater.*, 2011, **1**, 678.
13. Y. Zhao, L. Zhao, K. X. Yao, Y. Yang, Q. Zhang and Y. Han, *J. Mater. Chem.*, 2012, **22**, 19726.
14. Z. Zhang, J. Zhou, W. Xing, Q. Xue, Z. Yan, S. Zhuo and S. Z. Qiao, *Phys. Chem. Chem. Phys.*, 2013, **15**, 2523
15. M. Nandi, K. Okada, A. Dutta, A. Bhaumik, J. Maruyama, D. Derkx and Hiroshi Uyama, *Chem. Commun.*, 2012, **48**, 10283.
16. M. Saleh, J. N. Tiwari, K. C. Kemp, M. Yousuf and K. S. Kim, *Environ. Sci. Technol.*, 2013, **47**, 5467.
17. D. Lee, C. Zhang, C. Wei, B. L. Ashfeld and H. Gao, *J. Mater. Chem. A*, 2013, **1**, 14862.
18. M. Sevilla, C. Falco, M. M. Titirici and A. B. Fuertes, *RSC Advances*, 2012, **2**, 12792.

Table S5. Selectivity (S) for CO₂ of directly activated or conventionally activated carbons derived from sawdust biomass calculated using the IAST model.

Sample	IAST selectivity (S)
SD2600D	46
SD2600	47
SD2700D	42
SD2700	41
SD2800D	30
SD2800	29
SD4800D	23
SD4800	25

Selectivity (S) was calculated according to the equation; $S = n(\text{CO}_2) p(\text{N}_2)/(n(\text{N}_2) p(\text{CO}_2))$, where S is selectivity for CO₂, n is uptake of CO₂ or N₂ in mmol g⁻¹ at 0.15 bar and 0.85 bar, respectively, p(N₂) is 0.85 and p(CO₂) is 0.15).

Table S6. CO₂ uptake at 0 °C of directly activated or conventionally activated carbons derived from sawdust biomass

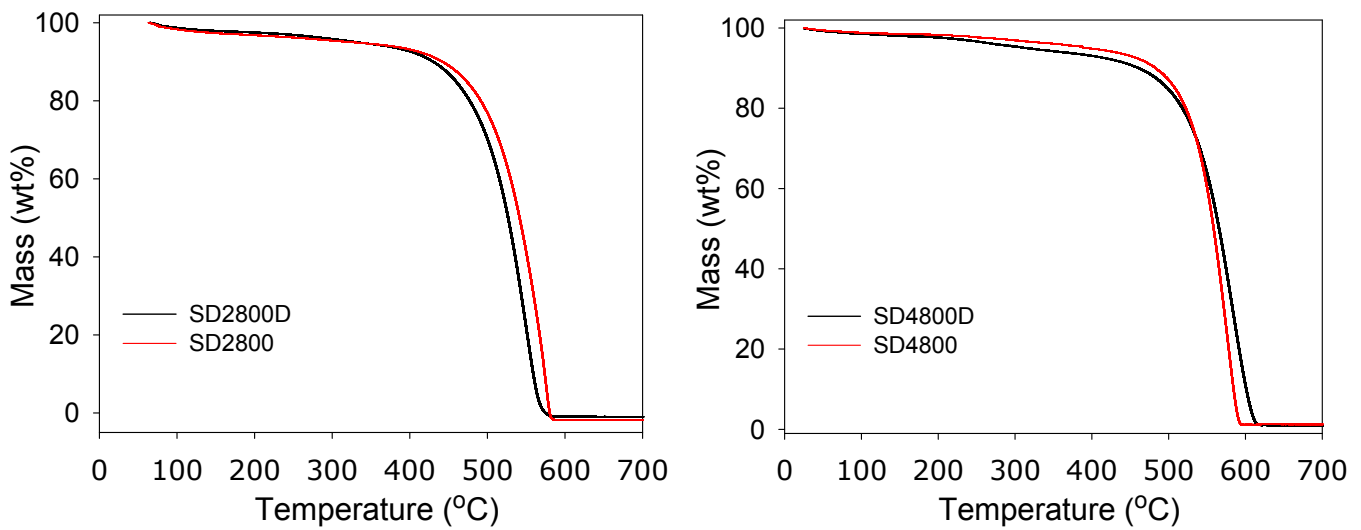
Sample	CO ₂ uptake ^a (mmol g ⁻¹)		
	0.15 bar	1 bar	20 bar
SD2600D	2.4	6.1	10.4
SD2600	2.5	6.6	11.2
SD2700D	2.6	7.3	13.4
SD2700	2.2	6.8	13.8
SD2800D	1.7	6.1	23.8
SD2800	1.5	5.8	21.7
SD4800D	1.1	4.8	30.3
SD4800	0.9	4.1	30.7

^aCO₂ uptake at 0 °C and various pressures (i.e., 0.15 bar, 1 bar and 20 bar).

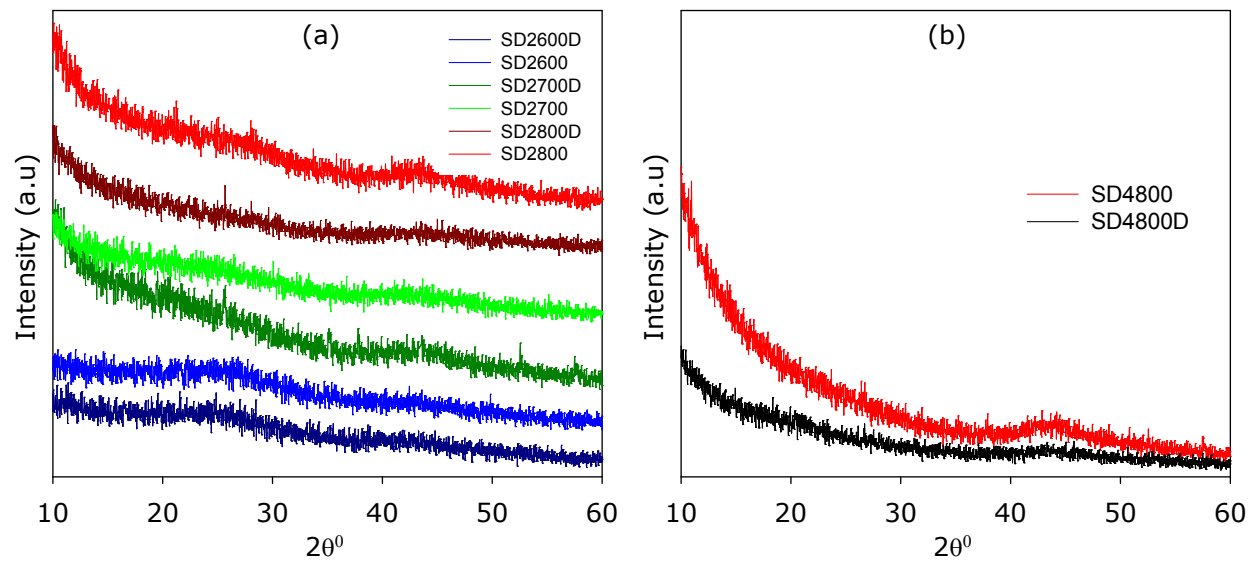
Table S7. CO₂ uptake at 0 °C and 1 bar of various carbons compared to study carbons.

Sample	CO ₂ uptake ^d (mmol g ⁻¹) at 1 bar	Reference
SD2600D	6.1	This work
SD2600	6.6	This work
SD2700D	7.3	This work
SD2700	6.8	This work
SD2800D	6.1	This work
SD2800	5.8	This work
SD4800D	4.8	This work
SD4800	4.1	This work
N-Doped microporous carbon	2.7	1
Microporous carbon	2.3	2
Microporous organic polymer	3.5	3
Covalent organic framework	4.0	4
Hollow octahedral carbon cage	4.0	5
Hierarchically porous carbon	4.6	6
N-Doped carbon monolith	4.2	7
Porous carbon sheets	4.3	8
NPCNS carbon	4.4	9

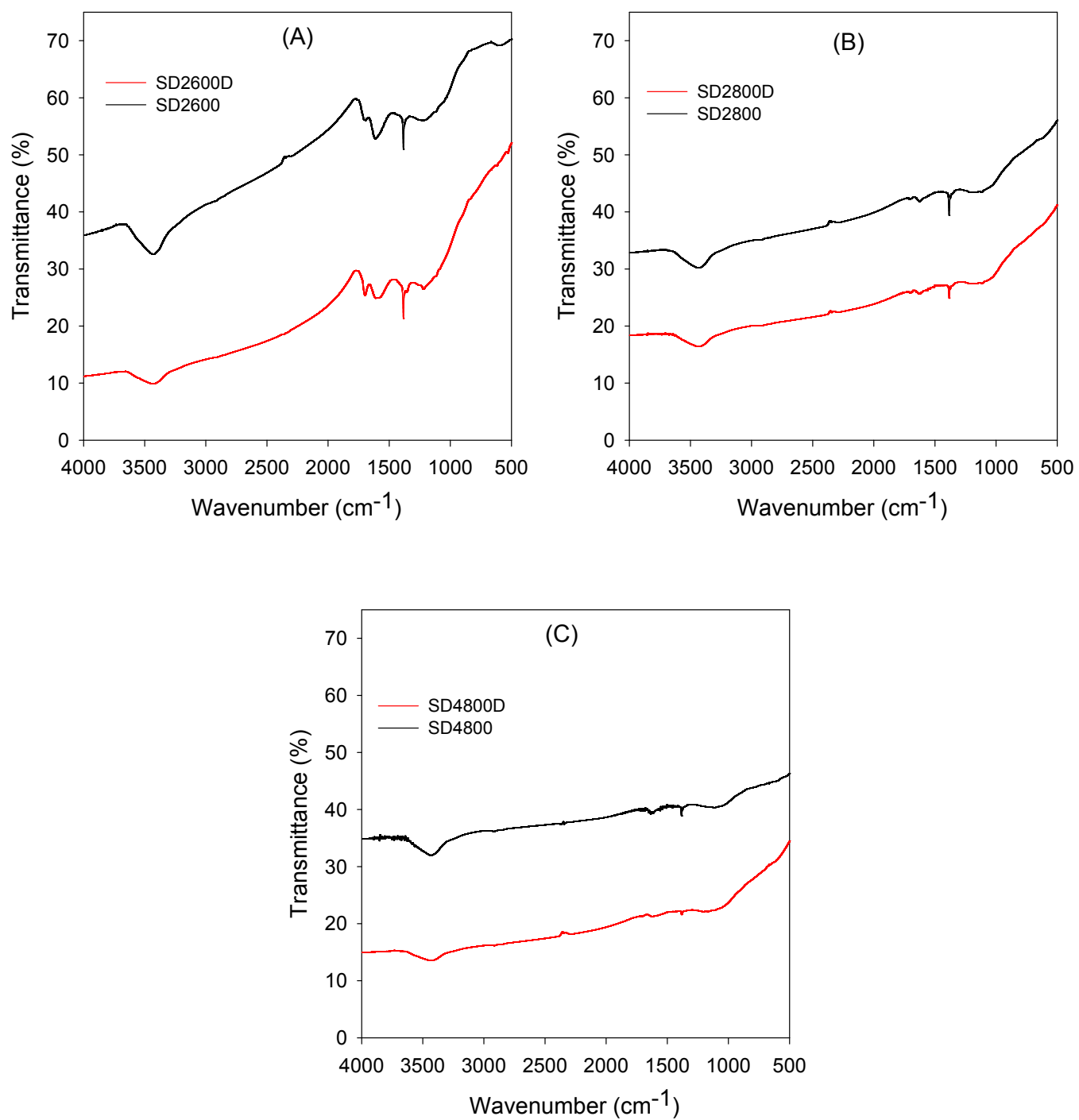
1. J. Wang, I. Senkovska, M. Oschatz, M. R. Lohe, L. Borchardt, A. Heerwig, Q. Liu and S. Kaskel, *ACS Appl. Mater. Interfaces*, 2013, **5**, 3160.
2. D. L. Sivadas, R. Narasimman, R. Rajeev, K. Prabhakaran and K. N. Ninan, *J. Mater. Chem. A*, 2015, **3**, 16213.
3. R. Du, N. Zhang, H. Xu, N. Mao, W. Duan, J. Wang, Q. Zhao, Z. Liu and J. Zhang, *Adv. Mater.*, 2014, **26**, 8053.
4. N. Huang, X. Chen, R. Krishna and D. Jiang, *Angew. Chem., Int. Ed.*, 2015, **54**, 2986.
5. A. Aijaz, J.-K. Sun, P. Pachfule, T. Uchida and Q. Xu, *Chem. Commun.*, 2015, **51**, 13945.
6. S. J. Yang, M. Antonietti and N. Fechler, *J. Am. Chem. Soc.*, 2015, **137**, 8269.
7. N. López-Salas, M. C. Gutiérrez, C. O. Ania, J. L. G. Fierro, M. L. Ferrer and F. del Monte, *J. Mater. Chem. A*, 2014, **2**, 17387.
8. G.-P. Hao, Z.-Y. Jin, Q. Sun, X.-Q. Zhang, J.-T. Zhang and A.-H. Lu, *Energy Environ. Sci.*, 2013, **6**, 3740.
9. J. Gong, H. Lin, M. Antonietti and J. Yuan, *J. Mater. Chem. A*, 2016, **4**, 7313.



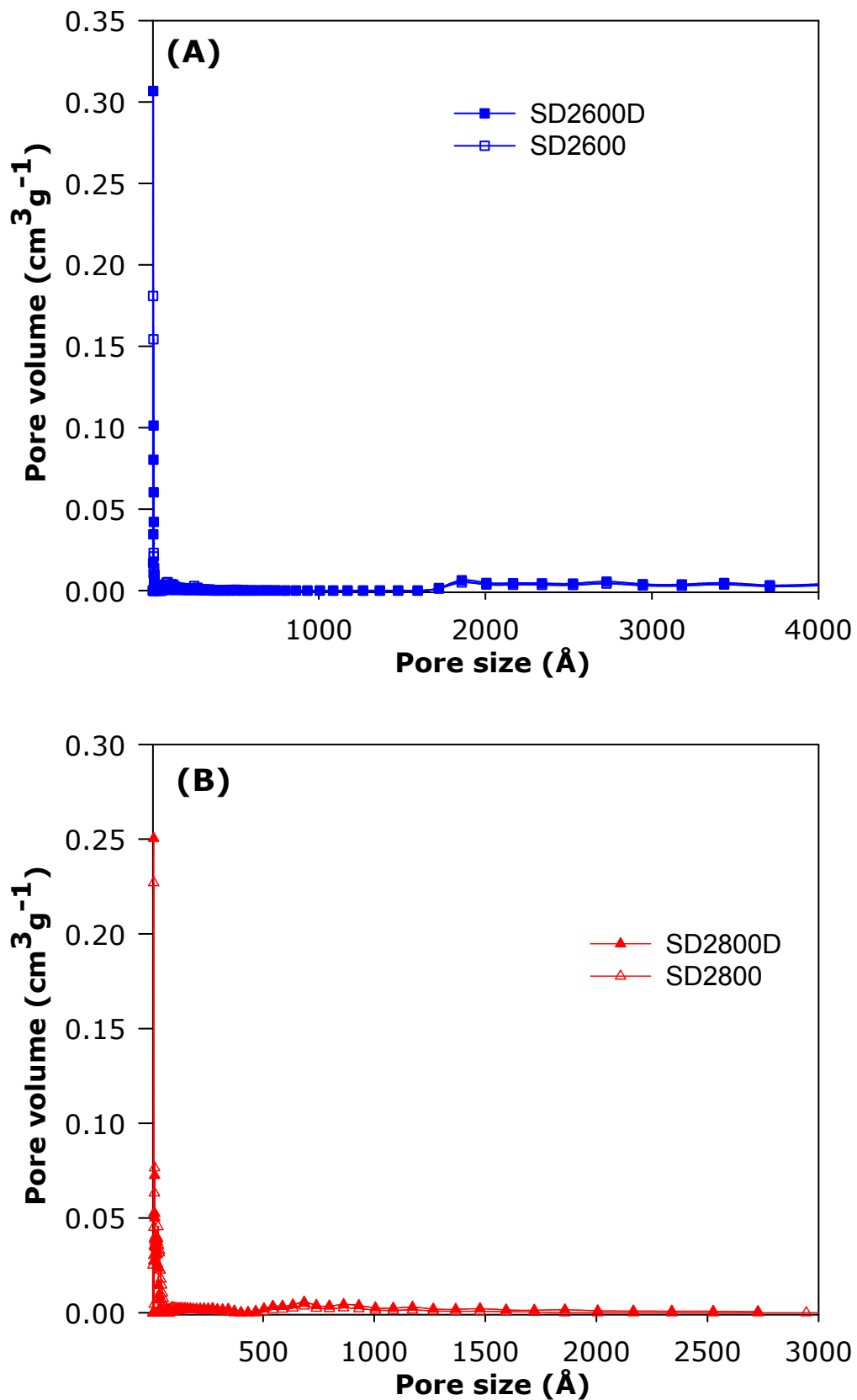
Supporting Figure S1. Thermogravimetric analysis (TGA) curve of sawdust-derived directly activated (SDxTD) or conventionally generated, via hydrothermal carbonisation, (SDxT) carbons.



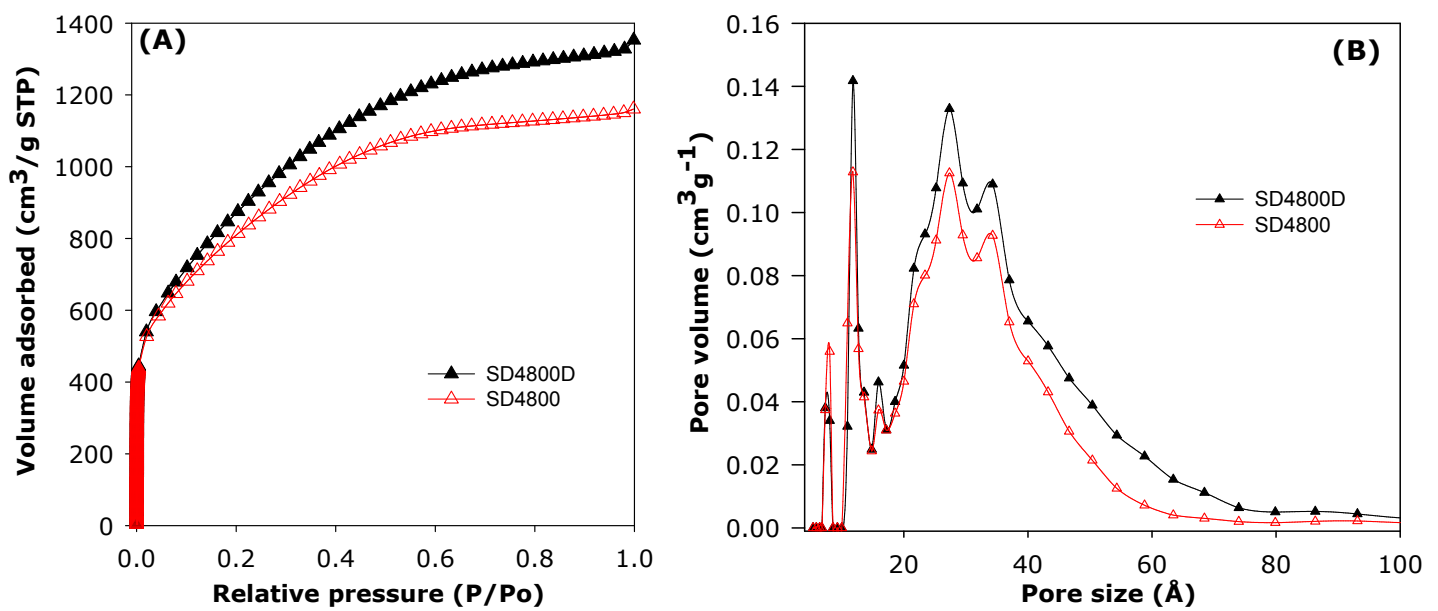
Supporting Figure S2. Powder XRD patterns of sawdust-derived directly activated (SD_xTD) or conventionally generated, via hydrothermal carbonisation, (SD_xT) carbons prepared at KOH/carbon ratio of (a) 2 or (b) 4.



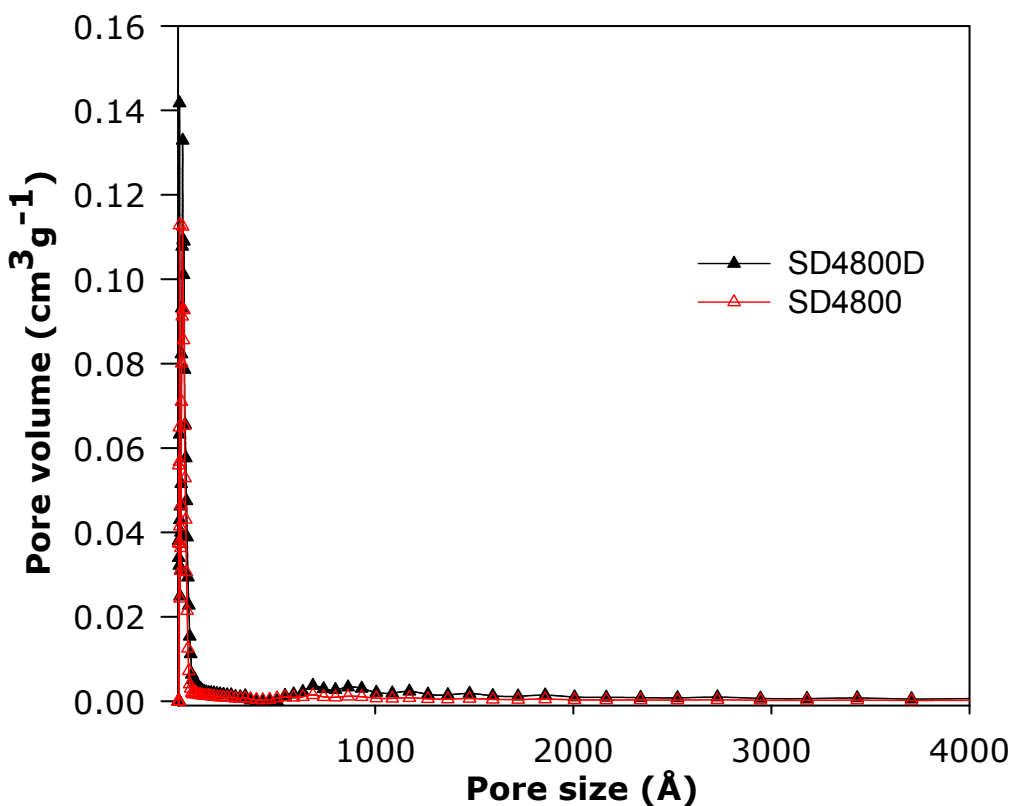
Supporting Figure S3. IR spectra of sawdust-derived directly activated (SD2TD) and conventionally generated (SD2T) carbons prepared at KOH/carbon ratio of 2 (A and B) or 4 (C) and various temperatures; (A) 600 °C, (B and C) 800 °C.



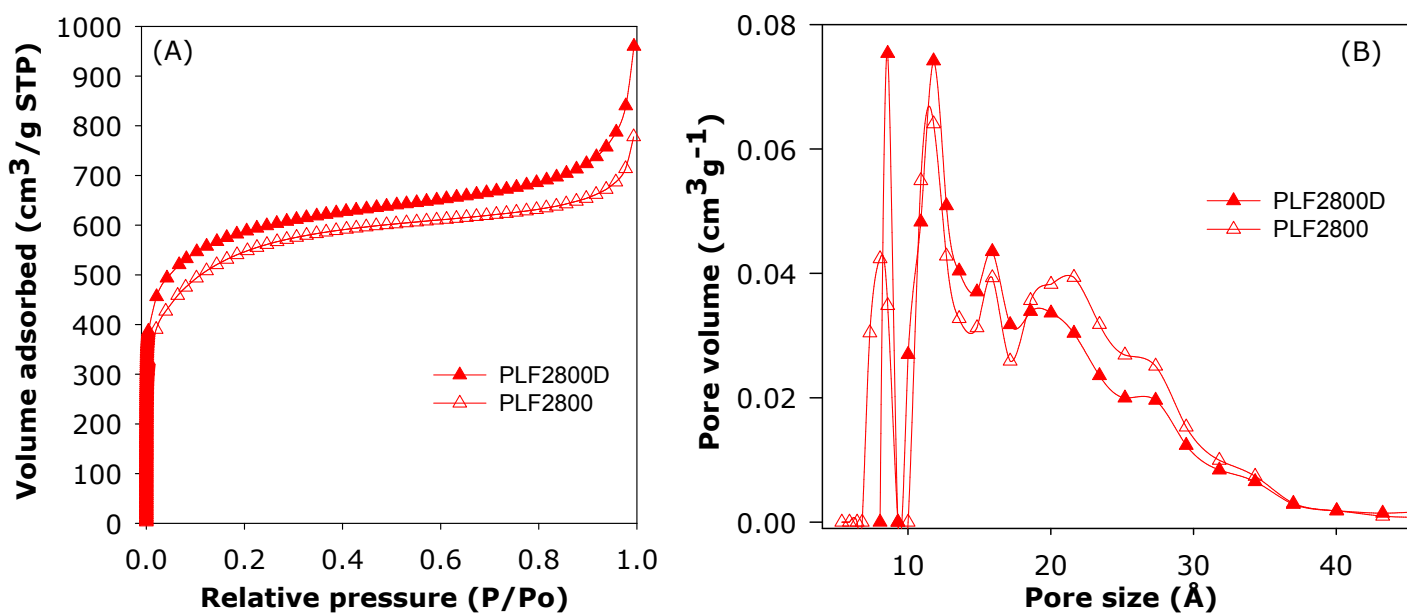
Supporting Figure S4. Pore size distribution of sawdust-derived directly activated (SD2TD) and conventionally generated (SD2T) carbons prepared at KOH/carbon ratio of 2 and (A) 600 °C or (B) 800 °C.



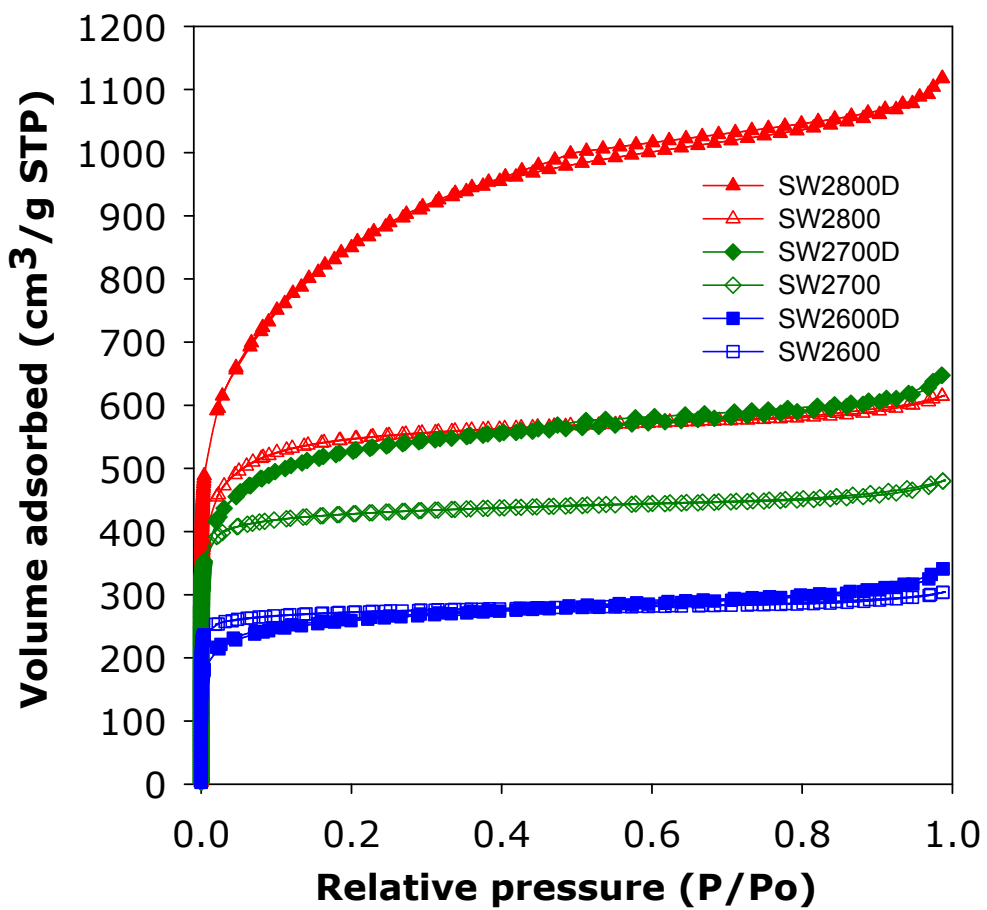
Supporting Figure S5. Nitrogen sorption isotherms (A) and corresponding pore size distribution curves (B) of sawdust-derived directly activated (SD4800D) or conventionally generated, via hydrothermal carbonisation, (SD4800) carbons prepared at 800 °C and KOH/carbon ratio of 4.



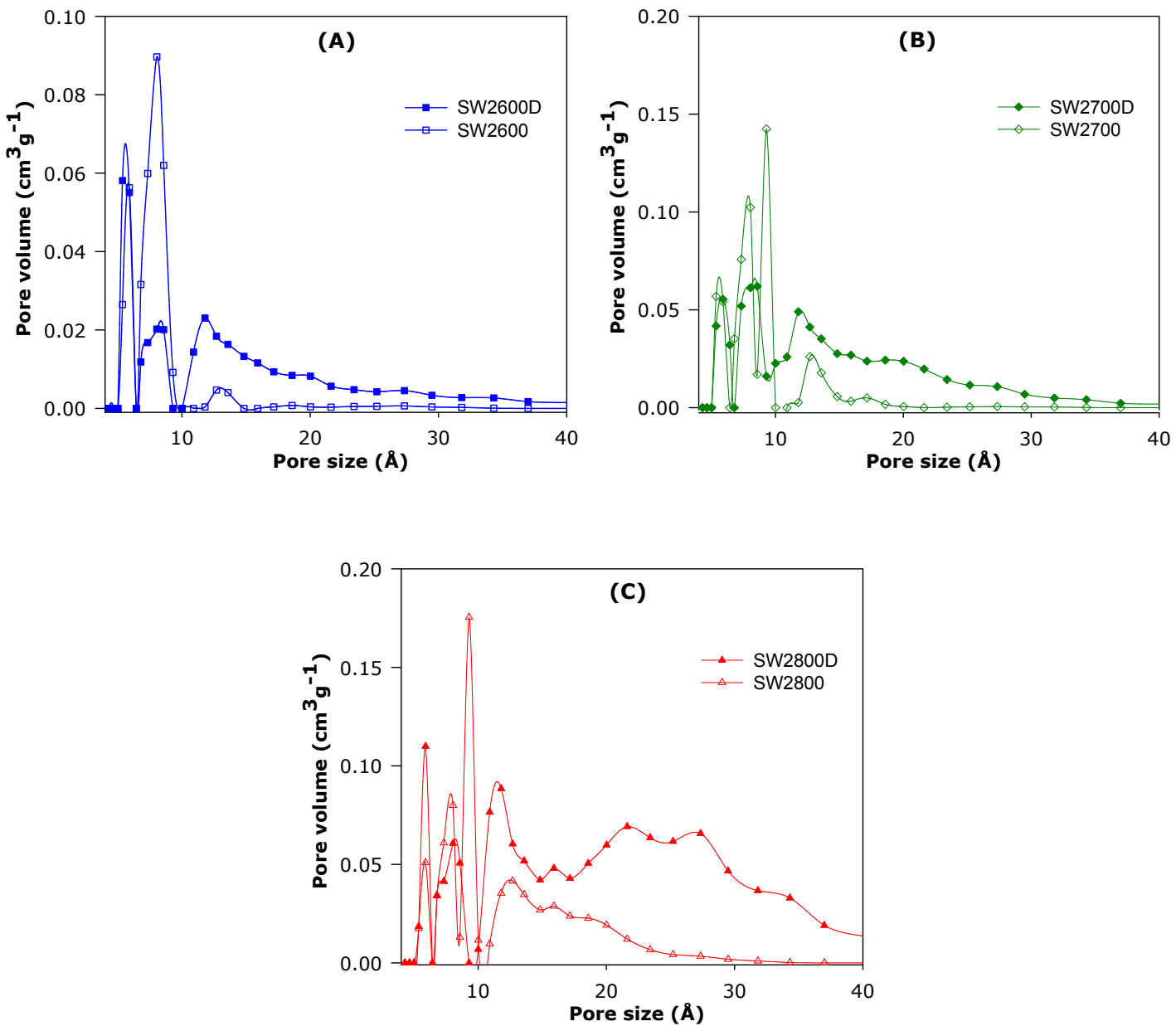
Supporting Figure S6. Pore size distribution curves of sawdust-derived directly activated (SD4800D) or conventionally generated, via hydrothermal carbonisation, (SD4800) carbons prepared at 800 °C and KOH/carbon ratio of 4.



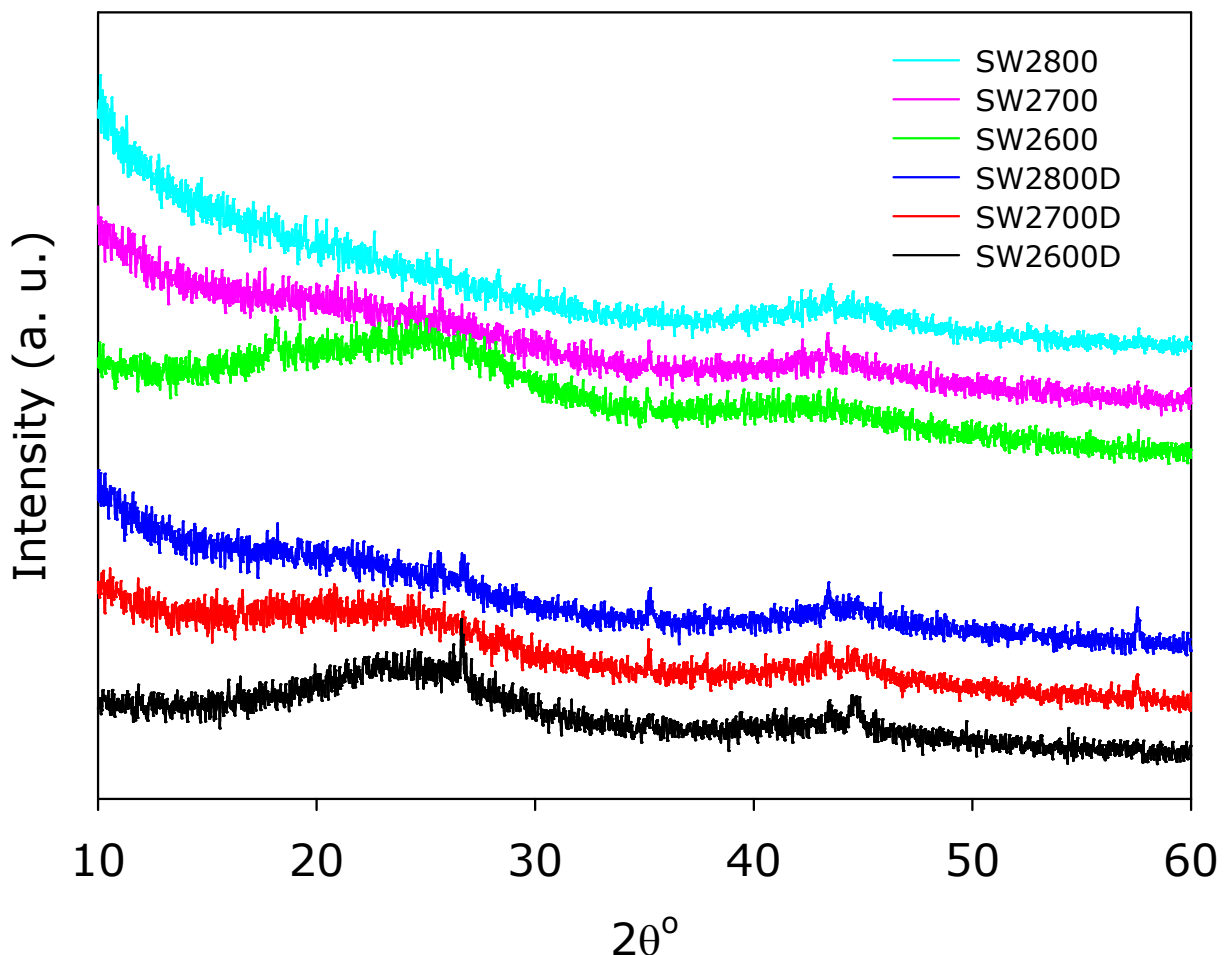
Supporting Figure S7. Nitrogen sorption isotherms (A) and corresponding pore size distribution curves (B) of directly activated (PLF2800D) or conventionally generated, via hydrothermal carbonisation, (PLF2800) carbons derived from the flowering plant *Paeonia Lactiflora*. The carbons were prepared at 800 °C and KOH/carbon ratio of 2.



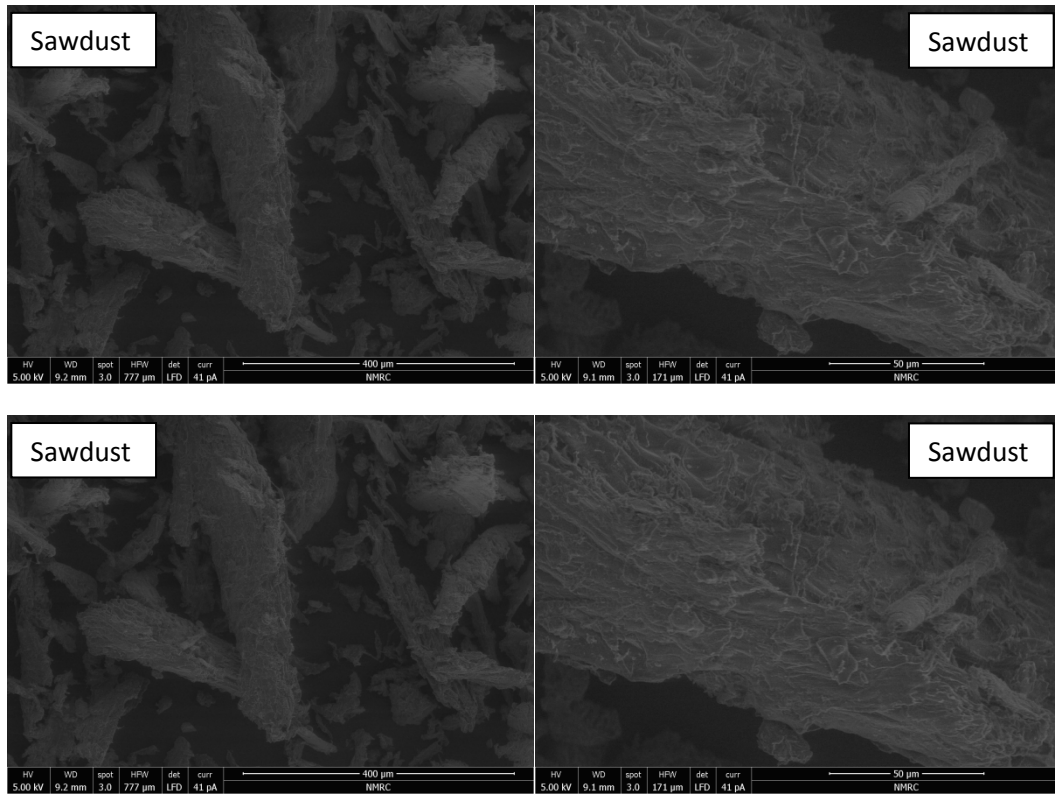
Supporting Figure S8. Nitrogen sorption isotherms of directly activated (SW2TD) or conventionally generated, via hydrothermal carbonisation, (SW2T) carbons derived from seaweed (*Sargassum fusiforme*). The carbons were prepared at KOH/carbon ratio of 2.



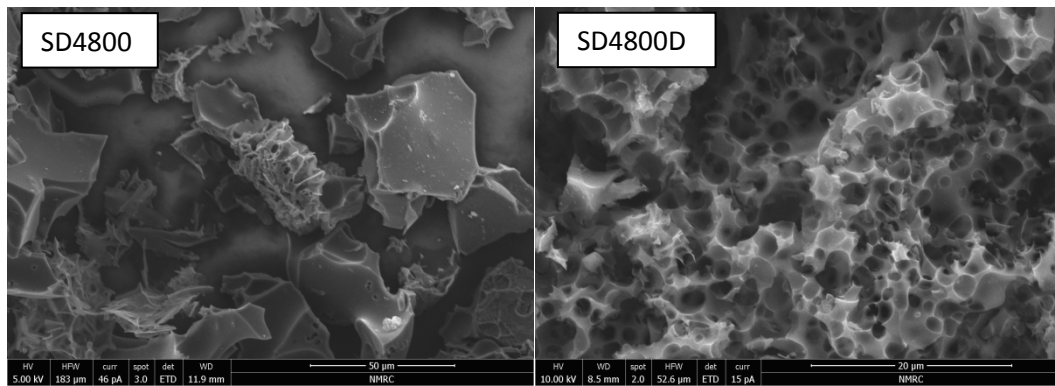
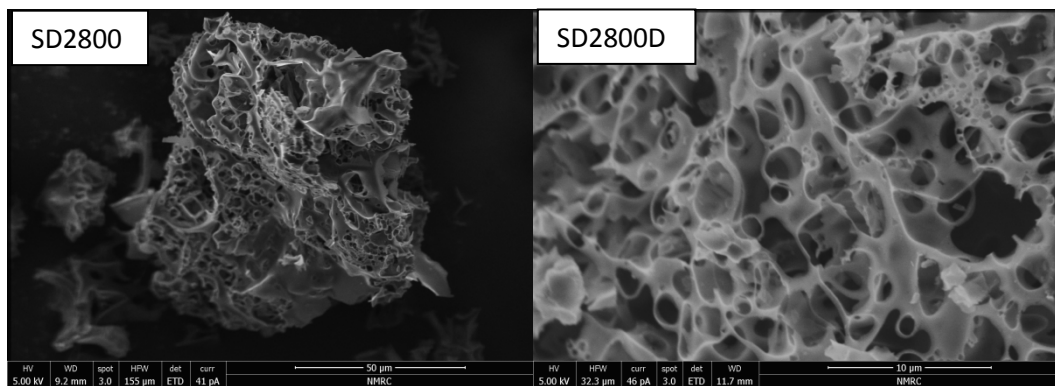
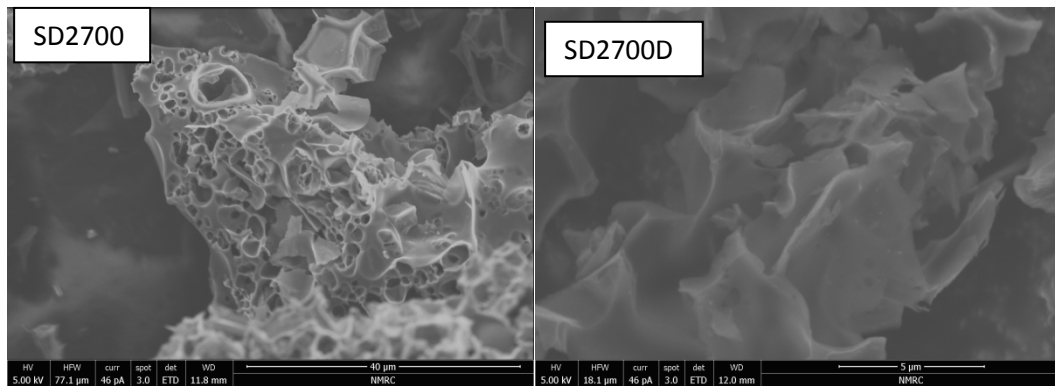
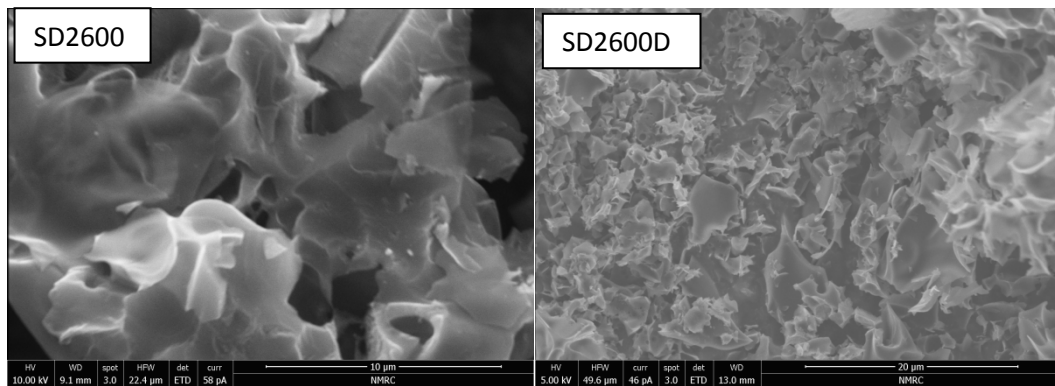
Supporting Figure S9. Pore size distribution curves of directly activated (SW2TD) or conventionally generated, via hydrothermal carbonisation, (SW2T) carbons derived from seaweed (*Sargassum fusiforme*). The carbons were prepared at KOH/carbon ratio of 2 and various temperatures; (A) 600 °C, (B) 700 °C and (C) 800 °C.



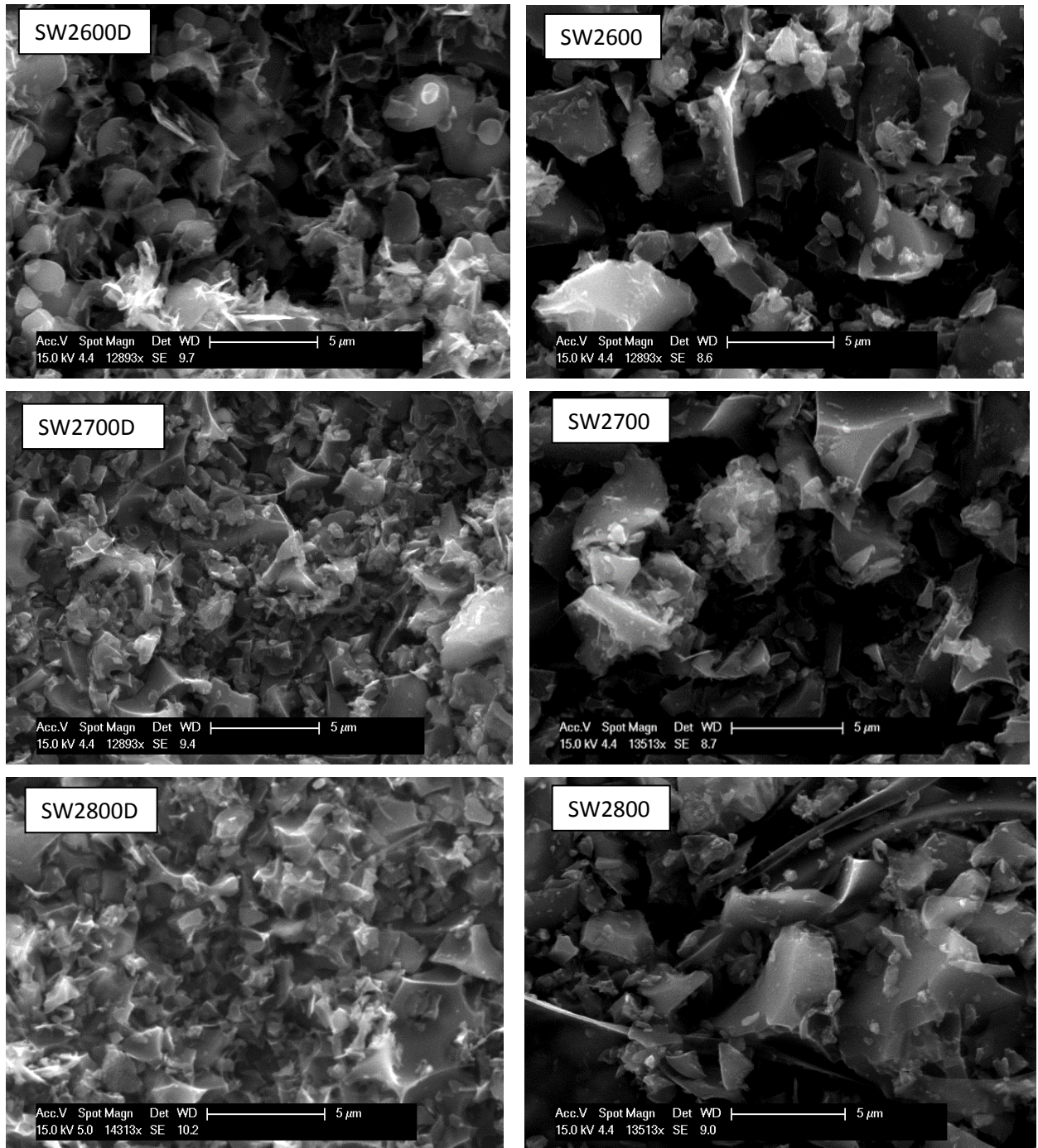
Supporting Figure S10. Powder XRD patterns of directly activated (SW2TD) or conventionally generated, via hydrothermal carbonisation, (SW2T) carbons derived from seaweed (*Sargassum fusiforme*). The carbons were prepared at KOH/carbon ratio of 2.



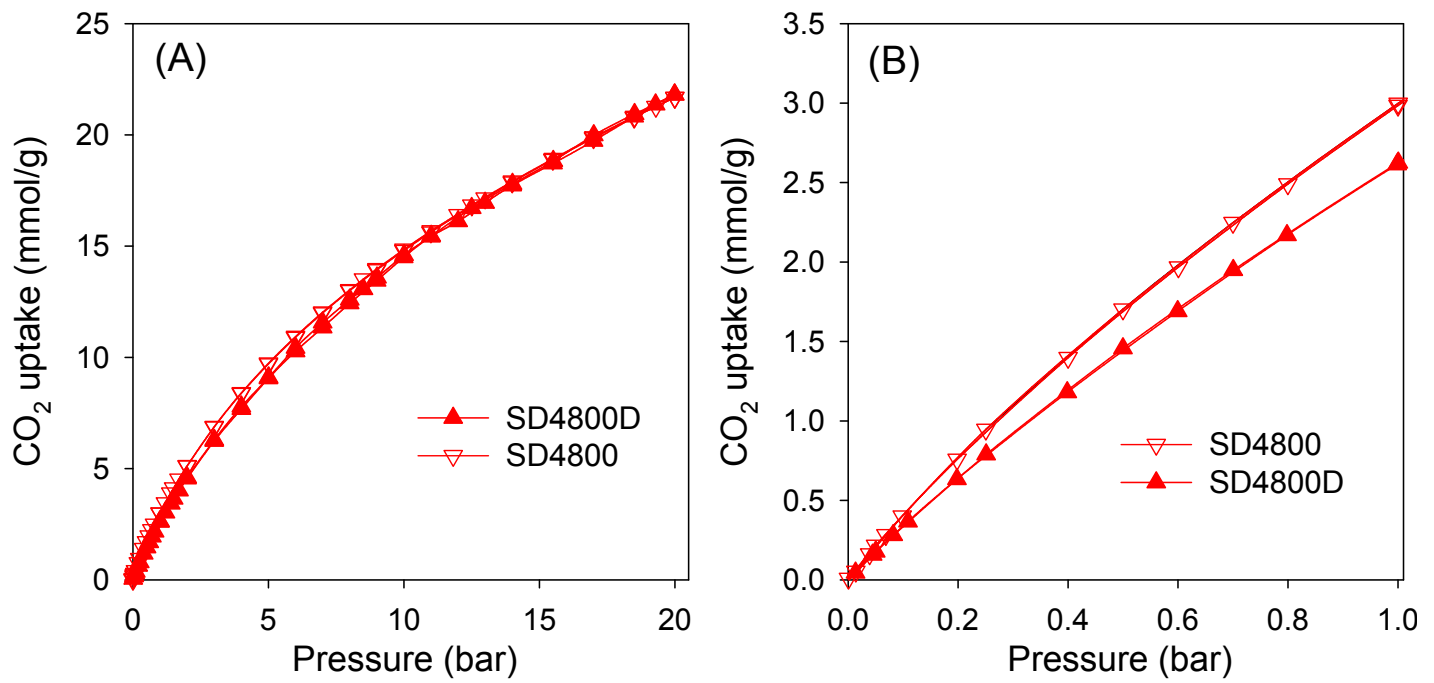
Supporting Figure S11. SEM images of raw sawdust.



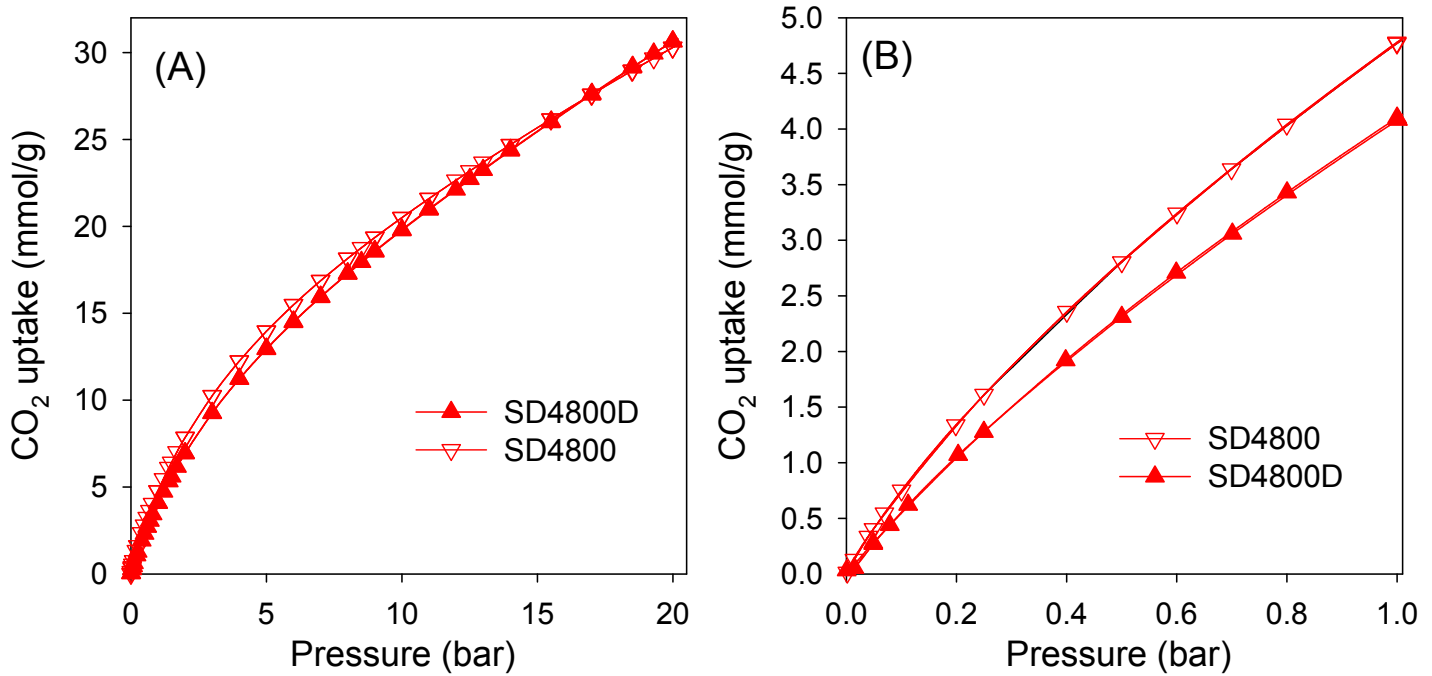
Supporting Figure S12. SEM images of sawdust-derived directly activated (SDxTD) or conventionally generated, via hydrothermal carbonisation, (SDxT) carbons.



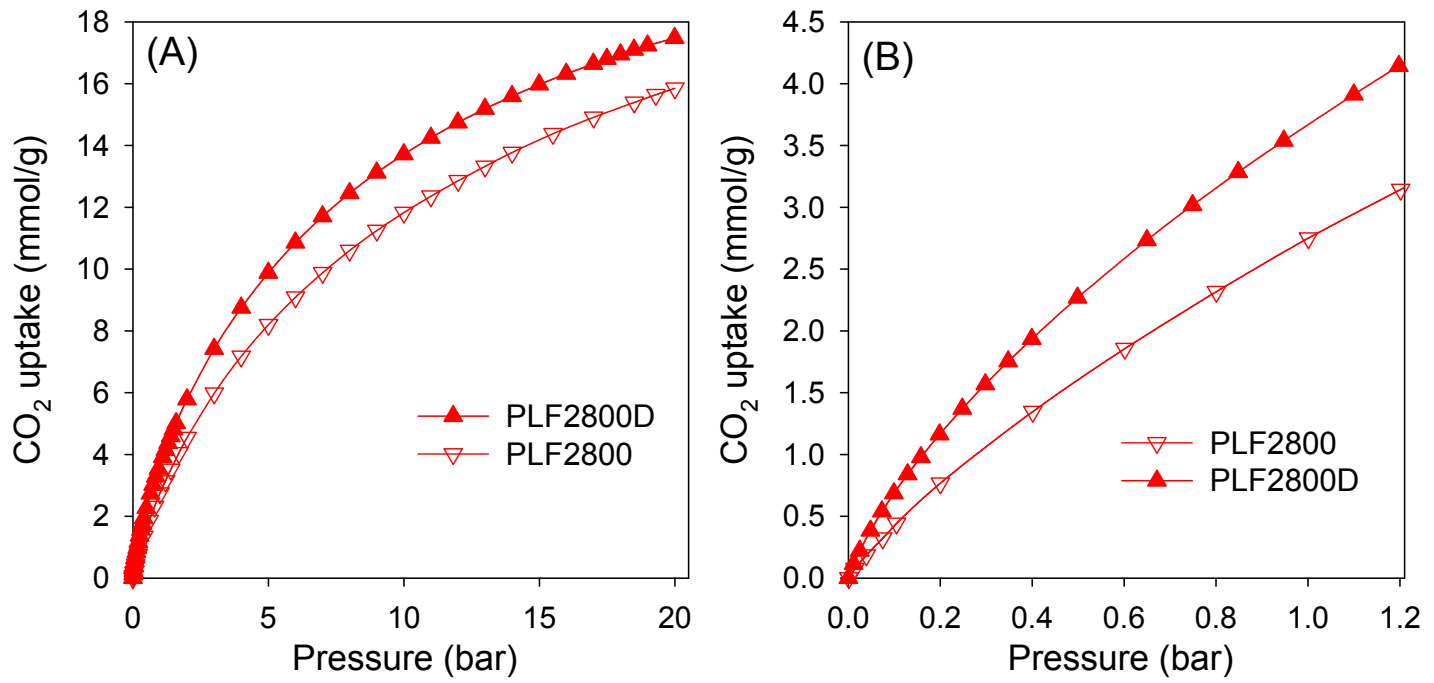
Supporting Figure S13. SEM images of directly activated (SW2TD) or conventionally generated, via hydrothermal carbonisation, (SW2T) carbons derived from seaweed (*Sargassum fusiforme*). The carbons were prepared at KOH/carbon ratio of 2.



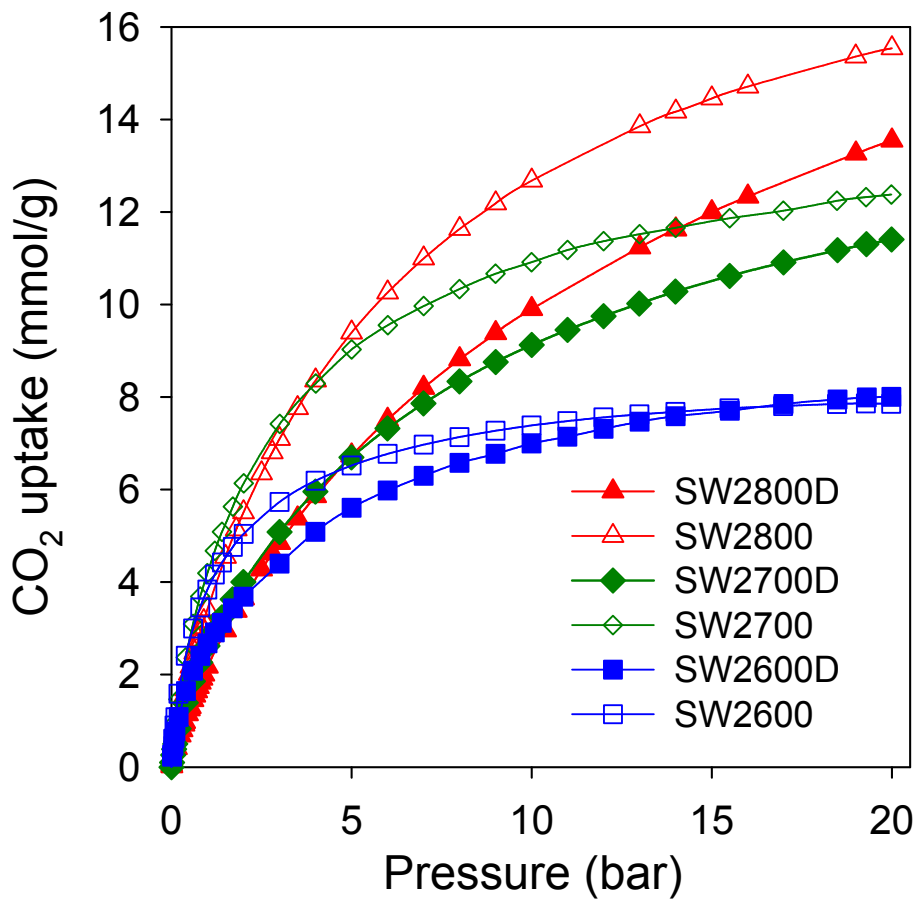
Supporting Figure S14. CO₂ uptake isotherms at 25 °C and 0 - 20 bar (A) and 0 – 1 bar (B) for sawdust-derived directly activated (SD4800D) or conventionally generated, via hydrothermal carbonisation, (SD4800) carbons prepared at 800 °C and KOH/carbon ratio of 4.



Supporting Figure S15. CO₂ uptake isotherms at 0 °C and 0 - 20 bar (A) and 0 – 1 bar (B) for sawdust-derived directly activated (SD4800D) or conventionally generated, via hydrothermal carbonisation, (SD4800) carbons prepared at 800 °C and KOH/carbon ratio of 4.



Supporting Figure S16. CO₂ uptake isotherms at 25 °C and 0 - 20 bar (A) and 0 – 1 bar (B) for directly activated (PLF2800D) or conventionally generated, via hydrothermal carbonisation, (PLF2800) carbons derived from the flowering plant *Paeonia Lactiflora*. The carbons were prepared at 800 °C and KOH/carbon ratio of 2.



Supporting Figure S17. CO₂ uptake isotherms at 25 °C and 0 - 20 bar (A) and 0 – 1 bar (B) for directly activated (SW2TD) or conventionally generated, via hydrothermal carbonisation, (SW2T) carbons derived from seaweed (*Sargassum fusiforme*). The carbons were prepared at KOH/carbon ratio of 2.